PCCP

Accepted Manuscript

ROYAL SOCIETY OF CHEMISTRY

www.rsc.org/pccp

Journal Name

RSCPublishing

ARTICLE

Droplet based microfluidics: spectroscopic characterization of Levofloxacin and its SERS detection

Cite this: DOI: 10.1039/xoxxoooooox

Received ooth January 2012,
Accepted ooth January 2012

DOI: 10.1039/xoxxoooooox

www.rsc.org/

I. J. Hidi,[a] M. Jahn,[a] K. Weber,[a,b] D. Cialla-May,[a,b*] and J. Popp[a,b]

Levofloxacin (Levo), a second generation fluoroquinolone, has both clinical and environmental relevance. Therefore, the implementation of fast, robust and cost effective techniques for its monitoring is required. Here, its spectroscopic characterization and its detection in aqueous environment were carried out using surface enhanced Raman spectroscopy combined with droplet based microfluidics. The Levo molecule interacts with the silver nanoparticles via the carboxylate group and it adopts an upright or slightly tilted orientation. Furthermore, it is shown that the presence of Cl^- ions has a strong influence on the enhancement efficiency of the Raman signal of the target molecule. Thus, for the determination of the limit of detection (LOD) the measurements were carried out in the absence of any electrolytes. The estimated LOD is ~ 0.8 µM and the linear dynamic window ranges between 1-15 µM. These results were achieved after the normalization of the SERS signal to the Raman mode at 230 cm^{-1}. This band was attributed to the ν(Ag-O) stretching and it accounts for the Levo molecules in the first layer on the Ag nanoparticles.

Introduction

Levofloxacin (Levo), also known as Levaquin or Tavanic, is a second generation fluoroquinolone widely used against infections caused by both gram negative and gram positive bacteria.[1-4] Similar to most antibiotics, the drug has concentration dependent bacteria killing properties. Thus, discussions are on-going concerning whether it should be administered as single high dosage or multiple low dosages.[5] Furthermore, the drug undergoes limited metabolism in the human body. More than 85% of the administered dose is eliminated in human urine as unchanged drug. The normal Levo concentrations measured in urine are around 1 mM after 6 hours from the administration of a 500 mg dose and drop to 1 µM after 72 hours.[6-9] This results in the undesired presence of the antibiotic in surface waters, wastewaters, sediments and ground water worldwide.[10-12] Therefore, the monitoring of Levo is of high importance for both clinical and environmental purposes.

The gold standard to detect Levo is chromatography coupled with different detection methods, such as fluorescence or mass spectrometry.[9, 13, 14] In spite of the great technological advance, chromatographic methods are available only in large medical and academic centres and reference laboratories due to the complexity of these methods. Therefore, a less complex and more readily available detection method is required.

The combination of microfluidic platforms with surface enhanced Raman spectroscopy (SERS) gained interest in the scientific community during the last years.[15-19] The method combines the fingerprint specificity of Raman spectroscopy[20-22] with the high sensitivity resulting from the excitation of plasmon resonances of the metallic nanoparticles[22-24]. Furthermore, high sample throughputs are achieved when instead of the conventional flow-through devices droplet based platforms are employed. Additionally, it was shown that quantitative detection with high reliability can be carried out either by using an isotope edited internal standard[25] or by employing the target analyte itself as a standard[26]. Therefore,

the technique presents a high potential for online drug monitoring.

Before detecting biologically relevant molecules in complex matrices, an understanding of the fundamental spectroscopic characteristics of the pure analytes is necessary. Several studies have been published concerning the vibrational characterization of different quinolones.[27-30] Among these, Neugebauer et al.[27] focused on the vibrational spectroscopic characterization of norfloxacin, whereas Gunesekaran et al.[29] performed the vibrational analysis as well as the description of the electronic structure and nonlinear properties of Levo. Both works provide valuable details, however, none is going beyond the conventional Raman or Fourier transform infrared spectroscopy. Concerning the detection of quinolones by means of SERS, the adsorption behaviour of pefloxacin (a 3rd generation quinolone never approved for clinical practice) on silver colloids prepared by the Creighton method was presented by Lecomte et al.[30] However, the preparation of the employed silver nanoparticles has to be carried out in the presence of an ice bath and the resulted colloids are known to be weakly stable.[30] Hence, this would present a high limitation for the online monitoring of any drug.

To the best of our knowledge, this is the first time when Levo is detected by means of SERS and insights concerning its adsorption behaviour and orientation on the surface of Ag metallic nanoparticles are provided. Here, silver nanoparticles were produced at room temperature according to the Leopold-Lendl protocol.[31] Furthermore, the detection in purified water by means of lab-on-a-chip SERS (LOC-SERS) is also carried out. The linearity of the SERS signal vs. the in droplet concentration of the target molecule is improved by using the Raman mode due to the Ag-O vibration located at 230 cm^{-1} as a standard.

Materials and methods

Chemicals and reagents

Levo (HPLC, 98%), silver nitrate (ACS reagent,≥ 99%), hydroxylamine hydrochloride (ReagentPlus, 99%) and sodium hydroxide have been purchased from Sigma Aldrich and used as received.

Sample preparation

Stock solutions of 1 mM concentration of Levo were prepared by solving the appropriate quantity of powder in purified water. The solutions were stored in the fridge at 4^0C and used within one week. Working solutions of 10^{-5} and 10^{-4} M were obtained by diluting the stock solutions with purified water and used on the day of preparation.

The silver colloids were prepared according to the Leopold-Lendl protocol.[31] Briefly, 0.1 mmol silver nitrate was added to a mixture of hydroxylamine hydrochloride (0.15 mmol) and sodium hydroxide (0.3 mmol) under vigorous stirring. The solution turned instantaneously to grey-yellow colour. Stirring was continued for 10 s.

Instrumentation

UV-Vis absorption spectra were recorded in the 200–800 nm spectral range with a Jasco V650 diode array spectrophotometer. The acquisition speed was set to 200 nm/min with a spectral resolution of 1 nm.

For Raman, SERS and LOC-SERS measurements a WITec Raman microscope (WITec GmbH, Ulm, Germany) was used. As excitation a continuous wave diode-pumped solid-state laser with a wavelength of 514 nm and a maximum output power of 100 mW measured before the objective has been employed (Cobolt™). The same objective (Zeiss EC "Epiplan" DIC, 20x, N.A. 0.4) was used for focusing the laser beam and collecting the backscattered light. During measurements a 600 lines/mm grating was employed with a spectral resolution of ~5 cm^{-1}. The detection was carried out with a thermo-electric cooled (down to -70^0 C) CCD detector with 1024x127 active pixels and a pixel size of 26 µm x 26 µm.

In the case of the reference Raman spectra of Levo powder and saturated aqueous solution the laser power at the sample surface was set to 2 and 95 mW, respectively. The plotted spectra are the average of five acquisitions with an integration time of 5 s each. Concerning the SERS spectra acquired in cuvettes a laser power of 35 mW and 1 s integration time with ten acquisitions was chosen.

In order to determine the limit of detection of Levo in aqueous solution a microfluidic platform (see **Figure 1**) was employed. A detailed description of the platform has been published elsewhere.[25] Briefly, the glass chip has six different inlets and one outlet. All reagents are pumped into the chip through a computer controlled pump system (neMESYS Cetoni). At the first unit Levo/H_2O droplets are generated in the continuous phase of the mineral oil. At the second unit the Ag nanoparticles and the 1M KCl solution or H_2O are dosed into the already existing droplets. The mixing of the analytes is assured by the two meandering channels. Furthermore, the microchannels were functionalized with octadecyltrichloro-silane in order to obtain a hydrophobic surface. As a result, a minimum wettability of the aqueous droplets is achieved leading to the exclusion of memory effects usually characteristic for flow through microfluidic platforms. The flow rates of mineral oil (10 nl/s), Ag nanoparticles (9 nl/s) and 1M KCl/H_2O (2 nl/s) were kept constant during the measurement.

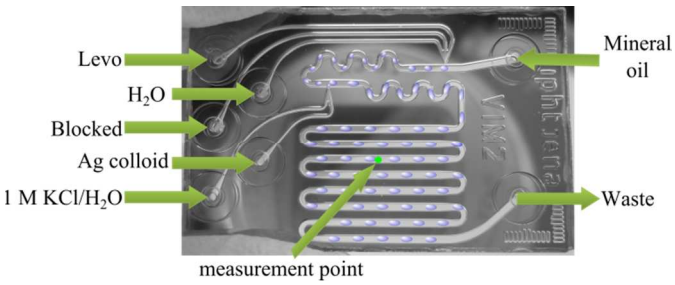

Figure 1 Picture of the droplet based microfluidic chip used for LOC-SERS measurements together with the depiction of the droplets and the inlets.

In order to have different in-droplet concentrations, the flow rates at the two ports of the droplet generator unit have been varied as follows: 0, 1, 2, 4, 6, 8, 10, 12, 14 nl/s for Levo and 14, 13, 12, 10, 8, 6, 4, 2, 0 nl/s for H_2O. For LOC-SERS measurements the chip was mounted on the microscope table. The SERS spectra were acquired continuously with 1 s integration time in the third channel. For every concentration step 1200 spectra were recorded containing pure droplet, pure mineral oil and also mixed spectra.

The theoretical Raman spectrum was calculated by employing the density functional theory (DFT) method. The theoretical frequencies were determined by using the B3LYP functional, 6-31G(d,p) basis set and a scaling factor of 0.97. The vibrational modes were assigned with the help of the Gauss-View molecular visualization program package.[32]

Results and discussions

Spectroscopic characterization of Levo

The chemical structure of Levo (full name: (S)-9-fluoro-2,3-dihydro-3-methyl-10-(4-methylpiperazin-1-yl)-7-oxo-7H-pyrido[1,2,3-de]-1,4-benzoxazine-6-carboxylic acid) is depicted in **Scheme 1**. Its main backbone is formed by the quinolone ring system having attached a fluorine atom and a piperazine moiety. The first one provides increased potency against organisms while the second one is responsible for pseudomonal activity.[28] The molecule exists as a zwitterion in the aqueous phase at the neutral pH range (pK_{a1}= 6.02 and pK_{a2} = 8.15)[33, 34] due to the presence of both anionic (carboxylic group) and cationic (piperazine ring) groups.

In **Figure 2** the reference Raman spectra measured on Levo powder and in the saturated aqueous solution is shown together with its calculated spectrum. In the case of the powder, the signal shows a high number of well-defined Raman modes. Most of the Raman bands involve the vibration of several atoms, their assignment to particular vibrational modes is difficult.[29] Nevertheless, the calculated Raman spectrum is in good accordance with the one presented by Gunesekaran et al.[29] Hence, the detailed vibrational assignment is not the subject of this publication.

By comparing **Figure 2 (a)** with **2 (b)** one may see that the signal of the molecules in an aqueous environment strongly differs from the one of the powder. This can be explained by considering that in the case of the solid state molecules form crystals. Singh et al.[35] performed the conformational analysis of

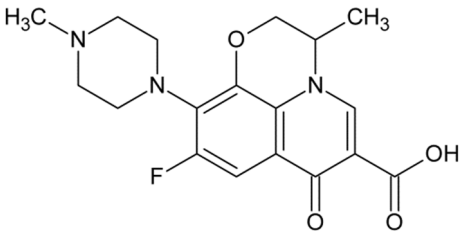

Scheme 1 Chemical structure of the Levo molecule ($C_{18}H_{20}FN_3O_4$).

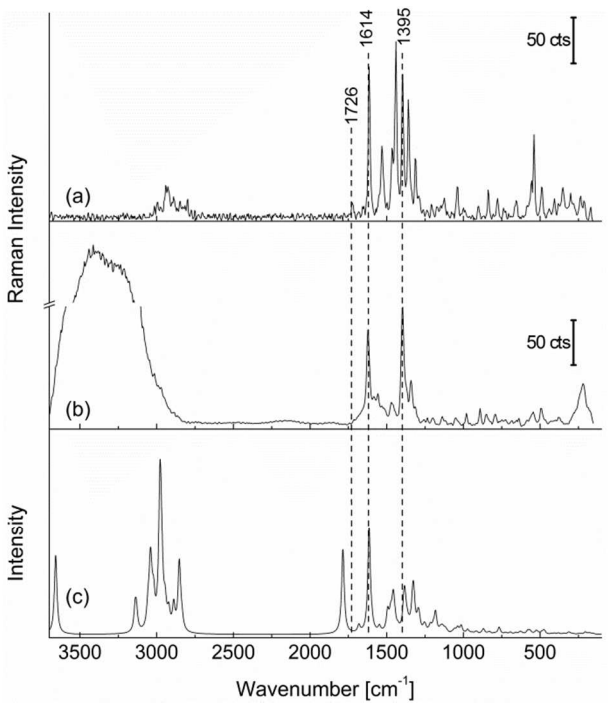

Figure 2 Recorded Raman spectrum of (a) Levo powder and (b) saturated aqueous solution. (c) Calculated Raman spectrum obtained using B3LYP /6-31 G(d,p) method.

the Levo molecule and they also predicted the crystal structure of the hydrated and anhydrous forms. According to their results, the molecular packing is obtained through strong π···π interactions and bridges formed via the O-H···N (N-methylpiperazine ring) and O-H···O (carboxylate group) hydrogen bonds.

Once Levo is solved in water the close packing might be destroyed inducing a change in the polarization and, hence, in the Raman spectrum. The Raman modes with the highest intensities present in the case of the saturated aqueous solution are centred at 1614 cm^{-1} and 1395 cm^{-1}. The first one is ascribed to the C=C vibration of the quinolone ring system while the second one is due to the combined contribution of the vibration of the same aromatic moieties with the COO^- symmetric stretching. The presence of the carboxylate group is due to the zwitterion characteristic of the molecules. Thus, upon protonation, the carboxylic unit converts into a carboxylate group. Here, the two C-O bonds have the same length with the negative charge centred equally on the two oxygen atoms rather than on the single bonded O. Hence, one may speak about the delocalization of electrons. This is also further supported by the very weak Raman mode at 1726 cm^{-1} assigned to the ν(C=O) vibration of the carboxylic group measured on powder. Nevertheless, the same band is completely absent in the aqueous solution as zwitterions are more stable as the uncharged Levo molecules.[34]

Generally, regardless of the preparation protocol, different salts are added to the Ag colloids in order to overcome the electrostatic repulsion between the particles.[31, 36, 37] As a result, a considerable enhancement of the SERS signal of the target

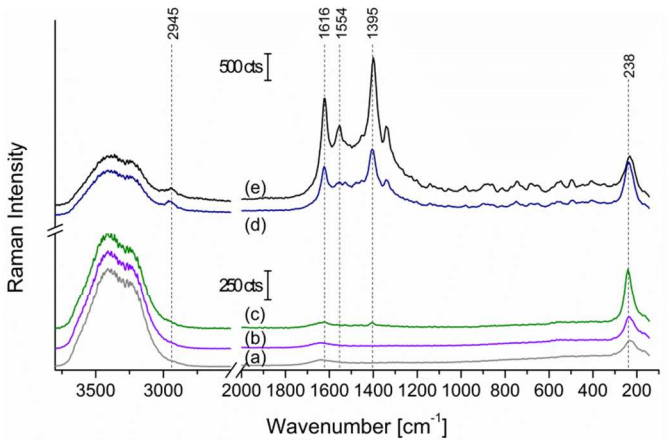

Figure 3 SERS spectra of (a) Ag + H_2O, (b) Ag + H_2O + 1 M KCl, (c) Ag + 1M KCl + Levo, (d) Ag + Levo + 1M KCl, (e) Ag + Levo + H_2O mixtures. The ratio of Ag colloids to Levo or H_2O was 1:1. The final concentrations of Levo and KCl in the mixture was $4.5 \cdot 10^{-5}$M and 0.9 mM, respectively.

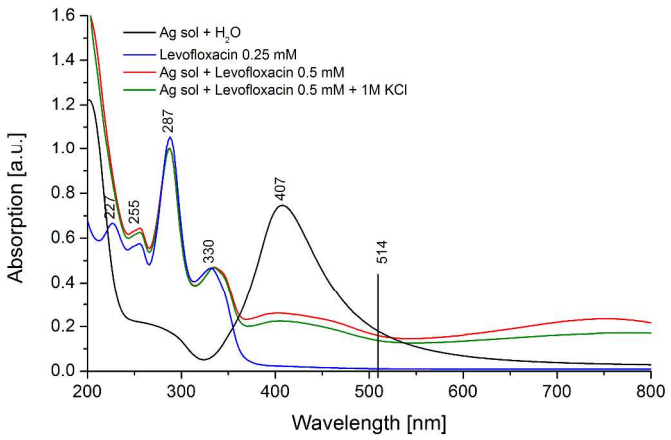

Figure 4 UV-Vis spectra of different solutions.

molecules is achieved. However, in the case of the Levo molecules the addition of potassium chloride induces the reverse effect. SERS spectra of different mixtures have been recorded and are presented in **Figure 3**. As reference, the blank spectra of Ag colloids with and without salt addition are also plotted. The presence of KCl in a final concentration of 0.9 mM results in the increase in the intensity of the band located around 238 cm^{-1} due to the absorption of Cl^- ions on the surface of the nanoparticles. Apart from this, only bands assigned to the vibrations of the water molecules are present. Hence, no interferences of the background are expected when the SERS spectrum of the analyte is acquired.

The influence of the salt addition on the SERS spectrum of the analyte is significant as it can be observed by comparing the spectra in **Figure 3 (c-e)**. The highest intensities were recorded when no electrolyte is added to the mixture. This may indicate that a so called "analyte induced aggregation" of the silver nanoparticles takes place. Nevertheless, the intensity strongly dropped when KCl was present in the solution. In both cases, the Levo molecules are allowed to interact with the Ag colloids, the 1M KCl being pipetted in the cuvette as last. Furthermore, when the salt is added first and only afterwards the analyte, the signal is almost completely disappearing. This phenomenon may be attributed to the strong affinity of the negatively charged chloride ions for the silver nanoparticles.[30, 38, 39] Consequently, a competition at the metallic surface takes place between the Levo molecules and the Cl^-. This is particularly proved by the importance of the order in which the target analyte and potassium chloride is added to the Ag nanoparticles.

The presented hypothesis is further supported by the recorded UV-Vis spectra. For reference, in **Figure 4** the extinction spectrum of the Ag colloid mixed with purified water in a ratio of 1:1 is presented. The absorption band centred at 407 nm is in good accordance with the already published results[31] proving that the synthesis was carried out with success. When Levo with a concentration of 0.5 mM is added to the Ag nanoparticles the colour of the colloid turns from yellow to grey. This is a clear indication for the induction of silver nanoparticle aggregates. Furthermore, in the recorded UV-Vis spectrum of the mixture one may see that the absorption band at 407 nm considerably decreases in intensity. Additionally, a second broad band centred at 750 nm appears in the high wavelength region due to the presence of silver clusters. Beside these, strong absorption bands located in the 200-350 nm region and assigned to the strong π-π* molecular transitions of the Levo molecule[29] were detected. The absorption spectrum of the pure analyte is plotted for reference with blue line in **Figure 4**. By further adding 1 M KCl solution to the Ag colloid:Levo mixture the intensity of the 407 nm absorption band and the one at 750 nm decreases further. This may indicate the creation of larger poli-dispersed Ag clusters which are no longer able to support plasmonic resonances, leading to the decrease of the SERS signal.

Furthermore, it is well known, that in order to obtain SERS spectra of the target analyte the molecules have to adsorb efficiently to the SERS substrate.[40] This occurs either via van der Waals forces or forces which involve valence bindings. In the first case no relevant differences are expected between the normal Raman and the SERS spectra. In the second case, the band intensities and positions can be affected due to the formation of metal-molecule complex. By closely comparing the normal Raman and SERS spectra (see **Figure 2** and **Figure 3**) no significant band shifts are noticed. However, the ratio of the two most intense Raman modes at 1395 and 1614 cm^{-1} is changing in the following way: for powder $I_{1395/1614}$= 0.98, for aqueous solution the ratio is 1.31, in the presence of silver nanoparticles it amounts to 1.33 while after KCl addition it increases to 1.47. The difference in the band ratio for the Raman spectra of powder and saturated aqueous solution arises due to the fact that the zwitterion is slightly more stable in aqueous environment than the uncharged form of the Levo.[34] As a result, the number of molecules with deprotonated carboxylic group increased. This leads to the disappearance of the 1726 cm^{-1} band ascribed to the C=O stretching and an

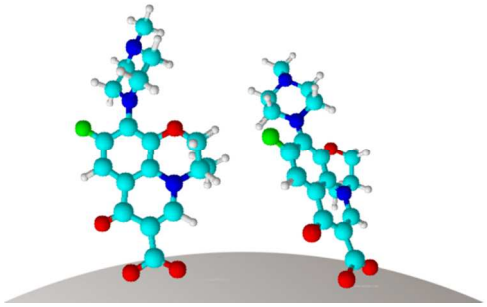

Scheme 2 Sketch of the orientation of the Levo molecule on the surface of the Ag nanoparticles.

increase in intensity of the 1395 cm^{-1} Raman mode. In the case of the SERS spectra, the change in band ratios was generally attributed to a change in the orientation of the target molecule. The two particular Raman modes have been ascribed to the stretching of the quinolone ring system with the difference that in the case of the 1395 cm^{-1} band the $\upsilon_s(COO^-)$ also has a contribution. This might suggest that the Levo interacts with the surface of the Ag nanoparticles through the COO^- group. Furthermore, the adsorption should happen via the lone pair electrons of the oxygen atom rather than through the delocalized electrons of the carboxylate group. The latter possibility is ruled out considering that the position of the band doesn't change as compared to the normal Raman spectrum.[41] In the literature shifts as high as 13-19 cm^{-1} have been observed when molecules containing carboxylate groups interact with the metallic surface via the delocalized electrons.[42, 43] Beside these considerations, the downshift by 10 cm^{-1} of the Raman mode at 238 cm^{-1} due to the ν(Ag-Cl) present in the SERS spectra when KCl is added might indicate the formation of Ag-O bonds instead of Ag-Cl.

Moreover, by taking into consideration the surface selection rules[44] one may deduce the orientation of a molecule containing aromatic moieties based on whether the in-plane or out-of-plane ring vibrations are predominantly enhanced. More exactly, when the Raman modes assigned to the in-plane ring vibrations are enhanced an upright orientation is assumed, while in the case of the enhanced out-of plane vibrations the molecule adopts a parallel orientation on the surface of the metallic nanoparticles. In the case of the SERS spectrum measured in the absence of KCl one may notice the presence of the Raman band centred at 1554 cm^{-1}. This was assigned to the in-plane mode of the of the quinolone ring system.[34] Furthermore, no out-of plane vibrations are detected in the 900-600 cm^{-1} region. As a result, it is assumed that the Levo molecules adopt an upright orientation with the aromatic ring system being perpendicular or slightly tilted on the Ag surface (see **Scheme 2**). When Cl^- ions are added to the solution, the 1554 cm^{-1} Raman mode loses intensity while no other new bands appear in the SERS spectrum as compared with the "no KCl" case. This might indicate that the target analyte is slightly tilted on the SERS substrate. This orientation is further supported by considering the Raman mode ascribed to the C-H stretching vibrations in the high wavenumber region (2945 cm^{-1}). It is well known, that these vibrations are more enhanced when the bond is perpendicular than when it lies parallel to the surface of the metallic nanoparticle.

LOC-SERS measurements

Due to the clinical and environmental relevance of Levo its detection in concentrations ranging between 1 mM to 1 μM or below is of major importance. Here, the first determination by means of LOC-SERS in the 1 – 100 μM range is presented. In order to provide reproducible measurement conditions and a high precision for serial dilutions a droplet based microfluidic setup has been used. According to the picture presented in **Figure 1**, aqueous solutions of Levo with a starting concentration of 10^{-5} and 10^{-4} M were mixed in the chip with purified water in order to obtain 15 different concentration steps. The time elapsed between the addition of the Ag colloids to the analyte containing droplet and measurement was 3 minutes. In **Figure 5** the mean SERS spectra of all concentration steps were plotted together with the blank spectrum. For the later one only purified water was pumped at the first dosing unit. When compared with this, the two Raman modes characteristic to Levo at 1395 and 1614 cm^{-1} are visible starting with a concentration of 1.42 μM. For a better visualization the band due to the quinolone ring stretching combined with $\nu_s(COO^-)$ mode was chosen. The peak area was calculated according to Simpson's rule and the mean value and its standard deviation were plotted against the in-droplet concentration of the target analyte (see **Figure 6**, black scatter plot). The calculation was performed for every single spectrum of a given concentration step.

For the low concentrations an exponential increase is observed, while for concentrations higher than 20 μM a plateau region was obtained. The latter phenomenon may be explained by considering the limited free binding sites at the Ag nanoparticles' surface. Once the amount of the Levo molecules reaches a critical threshold a further addition will not lead to the increase of the signal. Furthermore, the SERS effect has a short

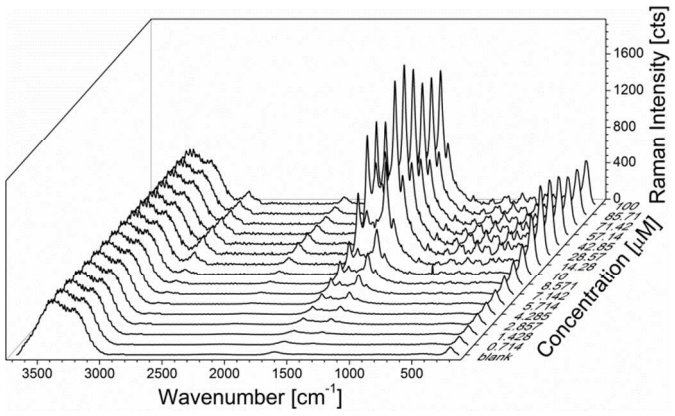

Figure 5 Mean SERS spectra of Levo with concentrations between 0.714 and 100 μM measured in the microfluidic platform. The mean spectrum of the blank (when only H_2O is pumped through at the first dosing unit) is also shown.

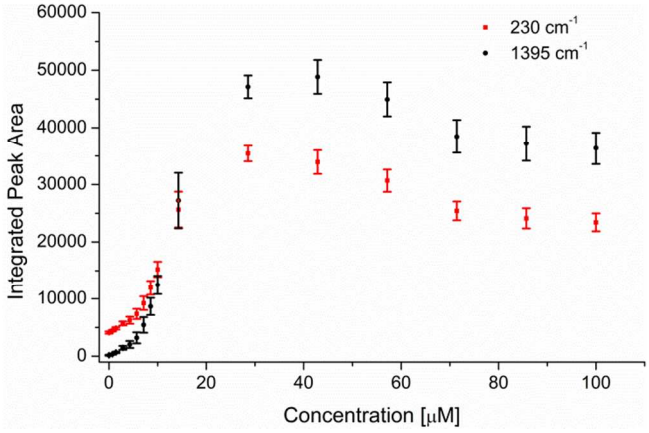

Figure 6 Concentration dependency of the integrated peak area for the Raman mode @ 1395 cm^{-1} due to the ring vibration of the quinolone system and ν(COO^-) and the @ 230 cm^{-1} due to the Ag-O stretching.

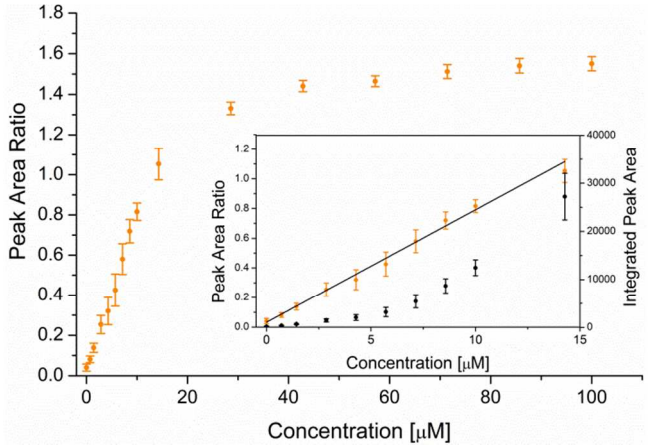

Figure 7 The peak area ratio of the 1395 cm^{-1} and 230 cm^{-1} Raman modes against the in-droplet concentration of Levo. In the inset, the comparison of the integrated peak area of the Raman mode at 1395 cm^{-1} vs. the normalized peak area is shown for the 0-15 μM concentration range.

range, the high electromagnetic field resulting from the excitation of plasmon resonances decays strongly with the distance. Therefore, only the molecules located in the first several layers on the metallic nanoparticles provide enhanced Raman signals.

Based on the fundamental characterization of the Levo molecule it was concluded that a so called analyte induced aggregation of the Ag nanoparticles takes place. Considering that no other molecules were present in the microdroplets, the intensity increase of the Raman mode centred at 230 cm^{-1} and assigned to the ν(Ag-O) is due to the increase of the number of adsorbed Levo molecules. Concerning the response of the peak area at the increase of the concentration a slightly different behaviour, as compared with the 1395 cm^{-1} band, is observed (**Figure 6,** red scatter plot). More exactly, for concentrations below 14 μM the increment for the $\upsilon(C=C)+\upsilon_s(COO^-)$ band is more pronounced. At 14 μM the two values are similar, while above this point both reach saturation. However, the peak area of the 230 cm^{-1} is smaller as compared with the other Raman mode. Therefore, the underlying mechanism behind the increment of the signal has to be different for the two Raman bands. On one hand, the Raman mode at 230 cm^{-1} band is due to the Levo molecules in the first layer on the surface of the metallic nanoparticles. On the second hand, the intensity of the 1395 cm^{-1} is increasing also due to the molecules present in the upper layers but still found in the hot-spot between the nanoparticles. Thus, for concentrations lower than 14 μM by calculating the peak area ratio of the two Raman modes a normalization of the SERS signal making use of the analyte induced aggregation can be carried out. In **Figure 7** it is shown that after the normalization a linear response with a correlation factor of 0.99 is achieved over the 0 – 15 μM concentration range (inset **Figure 7**). Furthermore, in order to calculate the limit of detection (LOD) the so called "three times standard deviation of the blank" IUPAC criterion was used. The same integration boarders applied for the calculation of the peak area of the Raman mode centred at 1395 cm^{-1} were used for calculating the area underneath the curve of the blank spectra. Afterwards, the value of the three times the standard deviation of the blank was used as threshold for estimating the LOD. According to this, concentrations down to 0.8 μM can be detected by employing the LOC-SERS technique.

Conclusions

In the present study, the spectroscopic characterization of the Levo molecule and its detection in the 1-100 μM concentration range in aqueous solution was carried out. It was shown that the aggregation of the silver nanoparticles is induced in the presence of the analyte and no additional salts are necessary in order to achieve high intensity SERS spectra. Furthermore, due to the competition at the surface of the Ag colloids between the Cl^- and the Levo molecules, the order in which these two chemicals are added to the silver sols has a high importance. Based on the surface selection rules, the change in the intensity ratio of selected Raman modes and the presence of the 230 cm^{-1} band ascribed to the ν(Ag-O) vibration the orientation of the molecule at the silver surface was determined. Thus, in the absence of chloride ions Levo adopts a perpendicular or slightly titled orientation, while in the presence of KCl it is titled. In both cases, the interaction of the analyte happens via the lone pair electrons of the oxygen atoms of the carboxylate group. In the second part of the paper it was shown that Levo can be detected in a concentration as low as 0.8 μM. Moreover, the linearity of the SERS signal vs. the in-droplet concentration of the analyte can be significantly improved by normalizing the signal to the Raman mode due to the Ag-O stretching vibration.

Acknowledgements

The funding of the PhD project of I.J. Hidi within the framework "Carl-Zeiss-Strukturmaßnahme" is gratefully acknowledged. The projects "QuantiSERS" (03IPT513A) and "Jenaer Biochip Initiative 2.0" (03IPT513Y) within the framework "InnoProfile Transfer – Unternehmen Region" are supported by the Federal Ministry of Education and Research,

Germany (BMBF). We thank the microfluidic group of the IPHT for providing the lab-on-a-chip devices for the measurements. Additionally, the help of Dr. Dirk Bender with the theoretical calculations is gratefully acknowledged.

Notes and references

[a] Friedrich Schiller University Jena, Institute of Physical Chemistry and Abbe Center of Photonics, Helmholtzweg 4, 07745 Jena, Germany.
[b] Leibniz Institute of Photonic Technology Jena, Albert-Einstein-Str. 9, 07745 Jena, Germany.
*corresponding author: dana.cialla-may@uni-jena.de

1. D. S. North, D. N. Fish and J. J. Redington, *Pharmacotherapy: The Journal of Human Pharmacology and Drug Therapy*, 1998, 18, 915-935.
2. A. P. Cardile, H. Briggs, S. R. Burguete, M. Herrera, B. L. Wickes and J. H. Jorgensen, *Diagn Microbiol Infect Dis*, 2014, 78, 199-200.
3. R. F. Grossman, P.-R. Hsueh, S. H. Gillespie and F. Blasi, *International Journal of Infectious Diseases*, 2014, 18, 14-21.
4. F. C. Adler-Shohet, M. Low J Fau - Carson, H. Carson M Fau - Girma, J. Girma H Fau - Singh and J. Singh, *The Pediatric Infectious Disease* 2014, 33, 664-666.
5. G. Cao, J. Zhang, X. Wu, J. Yu, Y. Chen, X. Ye, D. Zhu, Y. Zhang, B. Guo and Y. Shi, *Journal of Clinical Pharmacy and Therapeutics*, 2013, 38, 394-400.
6. F. M. E. Wagenlehner, M. Kinzig-Schippers, F. Sörgel, W. Weidner and K. G. Naber, *Int J Antimicrob Agents*, 2006, 28, 551-559.
7. A. A. Salem, H. A. Mossa and B. N. Barsoum, *Spectrochimica Acta Part A: Molecular and Biomolecular Spectroscopy*, 2005, 62, 466-472.
8. M. Rambla-Alegre, J. Esteve-Romero and S. Carda-Broch, *Journal of Chromatography B*, 2009, 877, 3975-3981.
9. H. Sun, H. Wang and X. Ge, *Journal of Clinical Laboratory Analysis*, 2012, 26, 486-492.
10. E. M. Golet, I. Xifra, H. Siegrist, A. C. Alder and W. Giger, *Environmental Science & Technology*, 2003, 37, 3243-3249.
11. D. Fatta-Kassinos, S. Meric and A. Nikolaou, *Anal Bioanal Chem*, 2011, 399, 251-275.
12. I. Senta, S. Terzic and M. Ahel, *Water Research*, 2013, 47, 705-714.
13. R. Cazorla-Reyes, R. Romero-González, A. G. Frenich, M. A. Rodríguez Maresca and J. L. Martínez Vidal, *Journal of Pharmaceutical and Biomedical Analysis*, 2014, 89, 203-212.
14. S. Siewert, *Journal of Pharmaceutical and Biomedical Analysis*, 2006, 41, 1360-1362.
15. R. Gao, N. Choi, S. I. Chang, S. H. Kang, J. M. Song, S. I. Cho, D. W. Lim and J. Choo, *Analytica chimica acta*, 2010, 681, 87-91.
16. M. Lee, K. Lee, K. H. Kim, K. W. Oh and J. Choo, *Lab on a chip*, 2012, 12, 3720-3727.
17. M. Wang, M. Benford, N. Jing, G. Coté and J. Kameoka, *Microfluidics and Nanofluidics*, 2009, 6, 411-417.
18. C. Rivet, H. Lee, A. Hirsch, S. Hamilton and H. Lu, *Chemical Engineering Science*, 2011, 66, 1490-1507.
19. L. Wu, Z. Wang, S. Zong and Y. Cui, *Biosensors and Bioelectronics*, 2014, 62, 13-18.
20. P. C. Ashok, M. E. Giardini, K. Dholakia and W. Sibbett, *Journal of Biophotonics*, 2014, 7, 103-109.
21. K. M. Marzec, T. P. Wrobel, A. Rygula, E. Maslak, A. Jasztal, A. Fedorowicz, S. Chlopicki and M. Baranska, *Journal of Biophotonics*, 2014, 7, 744-756.
22. J. Yang, L. Zhen, F. Ren, J. Campbell, G. L. Rorrer and A. X. Wang, *Journal of Biophotonics*, 2014, 9999, n/a-n/a.
23. D. Cialla, A. Marz, R. Bohme, F. Theil, K. Weber, M. Schmitt and J. Popp, *Anal Bioanal Chem*, 2012, 403, 27-54.
24. P. Negri and R. A. Dluhy, *Journal of Biophotonics*, 2013, 6, 20-35.
25. A. März, K. R. Ackermann, D. Malsch, T. Bocklitz, T. Henkel and J. Popp, *Journal of Biophotonics*, 2009, 2, 232-242.
26. E. Kammer, K. Olschewski, T. Bocklitz, P. Rosch, K. Weber, D. Cialla and J. Popp, *Physical Chemistry Chemical Physics*, 2014, 16, 9056-9063.
27. U. Neugebauer, A. Szeghalmi, M. Schmitt, W. Kiefer, J. Popp and U. Holzgrabe, *Spectrochimica Acta Part A: Molecular and Biomolecular Spectroscopy*, 2005, 61, 1505-1517.
28. Y. Wang, K. Yu and S. Wang, *Spectrochimica Acta Part A: Molecular and Biomolecular Spectroscopy*, 2006, 65, 159-163.
29. S. Gunasekaran, K. Rajalakshmi and S. Kumaresan, *Spectrochimica Acta Part A: Molecular and Biomolecular Spectroscopy*, 2013, 112, 351-363.
30. S. Lecomte, N. J. Moreau, M. Manfait, J. Aubard and M. H. Baron, *Biospectroscopy*, 1995, 1, 423-436.
31. N. Leopold and B. Lendl, *The Journal of Physical Chemistry B*, 2003, 107, 5723-5727.
32. A. Frisch, A. Nielsen and A. Holder, *Gaussian Inc., Pittsburgh, PA*, 2000.
33. I. Sousa, V. Claro, J. L. Pereira, A. L. Amaral, L. Cunha-Silva, B. de Castro, M. J. Feio, E. Pereira and P. Gameiro, *Journal of Inorganic Biochemistry*, 2012, 110, 64-71.
34. A. Lambert, J.-B. Regnouf-de-Vains and M. F. Ruiz-López, *Chemical Physics Letters*, 2007, 442, 281-284.
35. S. S. Singh and T. S. Thakur, *CrystEngComm*, 2014, 16, 4215-4230.
36. A. M. El Badawy, K. G. Scheckel, M. Suidan and T. Tolaymat, *Science of The Total Environment*, 2012, 429, 325-331.
37. I. J. Hidi, A. Muhlig, M. Jahn, F. Liebold, D. Cialla, K. Weber and J. Popp, *Analytical Methods*, 2014, 6, 3943-3947.
38. J. Aubard, E. Bagnasco, J. Pantigny, M. F. Ruasse, G. Levi and E. Wentrup-Byrne, *The Journal of Physical Chemistry*, 1995, 99, 7075-7081.
39. G. Lévi, J. Pantigny, J. P. Marsault and J. Aubard, *Journal of Raman Spectroscopy*, 1993, 24, 745-752.
40. E. C. Le Ru and P. G. Etchegoin, in *Principles of Surface-Enhanced Raman Spectroscopy*, eds. E. C. L. Ru and P. G. Etchegoin, Elsevier, Amsterdam, 2009, DOI: http://dx.doi.org/10.1016/B978-0-444-52779-0.00013-1, pp. 367-413.
41. Y. J. Kwon, D. H. Son, S. J. Ahn, M. S. Kim and K. Kim, *The Journal of Physical Chemistry*, 1994, 98, 8481-8487.
42. H. Park, S. B. Lee, K. Kim and M. S. Kim, *The Journal of Physical Chemistry*, 1990, 94, 7576-7580.
43. Y. J. Kwon, S. B. Lee, K. Kim and M. S. Kim, *Journal of Molecular Structure*, 1994, 318, 25-35.

44. M. Moskovits and J. S. Suh, *The Journal of Physical Chemistry*, 1984, 88, 5526-5530.